Structural Monitoring and Maintenance, *Vol. 5, No. 1 (2018) 93-110*
DOI: https:// doi.org/10.12989/smm.2018.5.1.093

Internal force monitoring design of long span bridges based on ultimate bearing capacity ratios of structural components

Ke Hu[1], Zheng Xie[2], Zuo-Cai Wang[*2,3], Wei-Xin Ren[2,3] and Lei-Ke Chen[1]

[1]*Anhui Transportation Holding Group Co., Ltd., Hefei 230088, China*
[2]*School of Civil Engineering, Hefei University of Technology, Hefei 230009, China*
[3]*New theory and technology research platform of bridge structure safety monitoring, Hefei University of Technology, Hefei 230009, China*

(Received November 14, 2017, Revised February 11, 2018, Accepted February 16, 2018)

Abstract. In order to provide a novel strategy for long-span bridge health monitoring system design, this paper proposes a novel ultimate bearing capacity ratios based bridge internal force monitoring design method. The bridge ultimate bearing capacity analysis theories are briefly described. Then, based on the ultimate bearing capacity of the structural component, the component ultimate bearing capacity ratio, the uniformity of ultimate bearing capacity ratio, and the reference of component ultimate bearing capacity ratio are defined. Based on the defined indices, the high bearing components can then be found, and the internal force monitoring system can be designed. Finally, the proposed method is applied to the bridge health monitoring system design of the second highway bridge of Wuhu Yangtze river. Through the ultimate bearing capacity analysis of the bridge in eight load conditions, the high bearing components are found based on the proposed method. The bridge internal force monitoring system is then preliminary designed. The results show that the proposed method can provide quantitative criteria for sensors layout. The monitoring components based on the proposed method are consistent with the actual failure process of the bridge, and can reduce the monitoring of low bearing components. For the second highway bridge of Wuhu Yangtze river, only 59 components are designed to be monitored their internal forces. Therefore, the bridge internal force monitoring system based on the ultimate bearing capacity ratio can decrease the number of monitored components and the cost of the whole monitoring system.

Keywords: bridge health monitoring; internal force monitoring; ultimate bearing capacity; component ultimate bearing capacity ratio; reference component ultimate bearing capacity ratio

1. Introduction

The concept of structural health monitoring was primarily proposed in the aerospace field. For instances, Housner *et al*.(1997) defined the structural health monitoring system as an effective way to get and process data from the operating state structure and evaluate the main performance indicators of the structure. Boller *et al*. (2009) defined structural health monitoring as a technique for recording, analyzing, locating and predicting structural loads and damage states through a range of sensing devices.

∗Corresponding author, Professor, E-mail: wangzuocai@hfut.edu.cn

http://www.techno-press.org/?journal=smm&subpage=7 ISSN: 2288-6605 (Print), 2288-6613 (Online)

In bridge engineering, during the long-term use of the bridge, the vehicle, wind, earthquake loads, environmental factors, and the continuous deterioration of the material itself, cause the results in varying degrees of damage and deterioration of the bridge structure. These injuries, if not be monitored and maintained in time, can cause serious consequences, such as bridge damage and collapse. In order to ensure the safety, practicability and durability of the bridge structure, it is necessary to strengthen the bridge health monitoring (Li and Li 2002). The early bridge health monitoring system was installed to monitor the damage development or bridge conditions. For instance, to monitor the development of the fractures, the remote monitoring system was installed in Michigan Street Bridge in Wisconsin (Fish and Prine 1996). In order to monitor the vehicle, wind, and temperature induced responses of the bridge, the real-time monitoring system was installed in British Foyle Bridge in Ireland (Sloan *et al.* 1992). At present, many bridge health monitoring systems have been successfully installed in many countries. Kister *et al.* (2005, 2007) used extrinsic fibre Fabry–Perot sensors to monitor the strains of a reinforced concrete bridge. Hong and Kim (2010) installed a bridge health monitoring system to monitor the acceleration of a concrete girder bridge. Brownjohn *et al*. (2016) described the structural health monitoring systems of short to medium span bridges in UK. In mainland China, Li *et al*. (2016) reviewed the backgrounds, motivations and recent history of structural health monitoring developments to various types of engineering structures, including bridges.

However, since the early bridge health monitoring system is relatively simple and the layout of the sensors are usually based on the experience. For a complete and complex bridge health monitoring system, it is necessary to design or optimize the layout of the sensors. For instance, Yi *et al*. (2011, 2012, 2014) made a thorough studies in the optimal sensor placement. In their studies, a novel methodology called the modified monkey algorithm was used to design the sensors arrays of the structural health monitoring system. Their method is very different from the conventional method and is simple to implement. Recently, Sun *et al*. (2006, 2011) developed a quantitative analysis method on the vulnerability of structure damage scenarios, and proposed their method to design the sensors layout of the health monitoring system of long-span bridges.

At present, the design of the bridge health monitoring system is still difficult to consider the actual failure process of structures under various loads. In this paper, in order to determine the internal force monitoring components, the method based on the ultimate bearing capacity ratio of the bridge component is developed. The proposed method is based on the ultimate bearing capacity analysis of the long-span bridge subjected to various combinations of loads, and finds out the high bearing components and the failure paths. Based on the ultimate bearing capacity of the structural components, the component ultimate bearing capacity ratio, the uniformity of ultimate bearing capacity ratio, and the reference of component ultimate bearing capacity ratio are then defined. Based on the quantitative analysis of the bearing capacity of the components, the high bearing components of the bridge structure can then be determined and designed as the monitoring components.

Finally, the proposed method is applied into the bridge internal force monitoring design of the second highway bridge of Yangtze river in Wuhu city. Through the ultimate bearing capacity analysis of the bridge in eight load conditions, the high bearing components are found based on the proposed method. The bridge internal force monitoring system is then preliminarily designed based on the high bearing components. The method proposed in this paper is limited to the internal force monitoring design of the bridge. The whole health monitoring system of the bridge should include other monitoring indicators, such as structural characteristics monitoring indicators, structural load monitoring indicators and so on.

2. Bridge internal force monitoring design method based on component ultimate bearing capacity ratio

2.1 Component ultimate bearing capacity ratio and reference component ultimate bearing capacity ratio

According to the ratio of the internal force of the bridge member to the strength of the corresponding section, the component bearing capacity ratio, the uniformity of the bearing capacity ratio, and reference component bearing capacity ratio can be defined. The bearing capacity ratio of each component in the structure subjected to various loads can be quantitatively determined.

The component bearing capacity ratio is defined as the ratio of the sectional internal force to the strength of the corresponding section.

$$r^e = \frac{Q}{Q_p} \tag{1}$$

where r^e represents the component bearing ratio, e is the number of components, Q and Q_p represent the sectional internal forces and the sectional strength of the component e, respectively.

The uniformity of the component bearing ratio can be defined as

$$d = \frac{\bar{r} + r^{\min}}{\bar{r} + r^{\max}} \tag{2}$$

in which, d is the uniformity of the bearing capacity ratio, and $\bar{r}$ is the mean of the component bearing ratio. $r^{\max}$ and $r^{\min}$ represent the maximum and minimum values of the component bearing capacity ratio.

The reference component bearing capacity ratio can be further defined as

$$r^0 = r^{\max} - d(r^{\max} - r^{\min}) \tag{3}$$

With the increase of load, the component bearing capacity ratio and the reference component bearing capacity are varied. When the bridge reaches the ultimate bearing capacity, the ratio of the internal force of the section to the corresponding section strength is defined as the ultimate bearing capacity ratio of the component. The corresponding reference component bearing capacity ratio is defined as the reference ultimate bearing capacity ratio, which yields

$$r_{\lim}^e = \frac{Q_{\lim}}{Q_p} \tag{4}$$

in which, $r_{\lim}^e$ represents the component ultimate bearing ratio, e is the number of components, $Q_{\lim}$ and Q_p represent the sectional internal forces when the bridge reach its ultimate bearing capacity and the sectional strength of the components e, respectively.

Similarly, the uniformity of the ultimate bearing capacity ratio is defined as

$$d_{\lim} = \frac{\bar{r}_{\lim} + r_{\lim}^{\min}}{\bar{r}_{\lim} + r_{\lim}^{\max}} \tag{5}$$

where $d_{\lim}$ represents the ultimate bearing capacity ratio, which is transformed into interval (0, 1], and $\bar{r}_{\lim}$ is the mean of the component ultimate bearing ratio. $r_{\lim}^{\max}$ and $r_{\lim}^{\min}$ represent the maximum and minimum values of the component ultimate bearing capacity ratio.

Similarly, the reference ultimate bearing capacity ratio is defined as

$$r_{\lim}^{0} = r_{\lim}^{\max} - d_{\lim}(r_{\lim}^{\max} - r_{\lim}^{\min}) \tag{6}$$

The above characteristic parameters provide the basic criteria to determine the high bearing components. If the ultimate bearing capacity ratio of component is higher than the reference ultimate bearing capacity ratio, the component can be considered as high bearing component, otherwise it is low bearing component. When the ultimate bearing capacity ratio is equal to 1, it means that the component has been failed and needs to be monitored.

2.2 Internal force monitoring design based on ultimate bearing capacity ratios

The basic idea of the proposed method is based on the ultimate bearing capacity analysis of the bridge under various loads, and finds out the high bearing components and the failure paths. Through the definition of component ultimate bearing capacity ratio and reference component ultimate bearing capacity ratio, the high bearing components of the bridge can be determined as the monitored components.

The ultimate bearing capacity of the bridge due to static loads can be analyzed by using finite element method. The geometric and material nonlinearities need to be considered in the ultimate bearing capacity analysis of long span bridges (Bruno and Grimaldi 1985, Ren 1999, Roschke and Pruski 2000). In this paper, the finite element method is used to solve the ultimate bearing capacity of the structure considering the geometric and material nonlinearity. In the final solution of the algebraic equations, the arc length method is used to solve the problem iteratively, and the displacement criterion is used to determine the convergence.

To calculate the ultimate bearing capacity of the bridge due to dynamic loads, such as seismic load, the seismic elastic-plastic time history analysis method is used. In this paper, the direct integral method is used to solve the numerical solution of the elastic-plastic dynamic equation of the earthquake (Nazmy and Abdel-Ghaffar 1990, Ren and Obata 1999, Nazmy 2003). For the structural dynamic response analysis under the earthquake load, the time t can be divided into many tiny time periods Δt, and the numerical solution is obtained by numerical integration of the dynamic equation. In this paper, the Newmark method in the numerical integration method is used.

Through the analysis of the ultimate bearing capacity of the bridge under various loads, the weakest components due to various loads can be found. When the structure under a certain load condition, the external load increases, causing a component failure, it will bear the load redistribution to the adjacent component, and the redistribution of internal force, until the destruction of the whole structure. On the failure path, the ultimate bearing capacity ratio of components is 1, which is the weakest part of the structure. The component on the failure path is also the most vulnerable component of the bridge and designed as the monitored components in this paper.

3. Ultimate bearing capacity analysis of the second highway bridge of Wuhu Yangtze river

3.1 General introduction of the bridge

The span arrangement of the second highway bridge of Wuhu Yangtze river is (100+308+806+308+100) m. The bridge is a twin towers and cable-stayed bridge. The standard cable distance is 16 m. The longitudinal slope of the bridge is 1.98%. They are total 396 cables. The cable is used the saddle anchorage system at the top of the tower, and the lower end of the cable is anchored on the two sides of the girder. The main girder is a steel box girder. The bridge deck adopts the orthotropic bridge panel, and Q345 steel is used. The main girder is made up of two 18 m wide single box girders. The 17 m wide crossbeam is connected to the two main box girders. The total width of the bridge is 53 m, and the height of the main girder is 3.5 m at the middle span. The tower is divided into three parts, the upper, the middle, and the lower parts. The height of the upper tower is 108m, the height of the middle tower is 104.94 m, and the height of the lower tower is 46.540 m. The total height of the bridge tower is 259.48 m.

3.2 Finite element model

According to the design drawing of the second highway bridge of Wuhu Yangtze river, the finite element model of the bridge is established using the commercial software ANSYS. The bridge model is divided into 819 nodes, 833 elements, 7 kinds of material characteristics and 116 kinds of real constants. The tower and girder are simulated by using beam element BEAM188, and the piers are simulated using element BEAM4. The cable is simulated by the spatial bar element LINK180. The bottom of the tower is fully fixed. The origin of the coordinate system is selected at the edge of the steel box girder, along the longitudinal direction of the bridge is X axis, the transverse axis is Y axis, and the vertical axis is Z axis. The finite element model is shown in Fig. 1.

To calculate the ultimate bearing capacity of the second highway bridge of Wuhu Yangtze river, total eight load conditions are considered, which are presented in Table 1. Based on the design of the bridge, the live vehicle load is selected from the 'General Specifications for Design of Highway Bridges and Culverts (JTG D60-2015)"', and the wind load is selected from the 'Wind-resistant Design Specification for Highway Bridges (JTG D60-01-2004)'. The seismic load is selected E1 earthquake load which represents 475 year return period. The eight load cases are, load cases 1 to 4 consider dead load and n×(live vehicle load) at various distribution, load cases 5 and 6 consider dead load, live vehicle load, and n×(tailwind load /crosswind load), and load cases 7 and 8 considered dead load and n×(longitudinal /transverse E1 earthquake). Among them, n is the load amplification factor.

3.3 Ultimate bearing capacity analysis

The ultimate bearing capacity of the bridge is analyzed in the eight load conditions listed in Table 1, and the stresses of the bridge are obtained. The obtained stress is the principal stress of the element section. When the structure reaches the ultimate state, the load amplification factor n of the eight load cases 1 to 8 are 14.20, 8.67, 11.65, 14.52, 50.12, 26.24, 5.09, 3.92, respectively.

The stress of cables in eight load conditions is presented in Fig. 2. For the load case 1, the stress

of cable J25 in the mid-span approaches the yielding stress. The stress value of the cable in the edge pier area, the mid-span of the side span and the 1/4 span are large, which is presented in Fig. 2(a). For the load case 2, the stress value of the cable A20 in the auxiliary pier area is large, and the stress approaches yielding stress, which is presented in Fig. 2(b). As shown in Fig. 2(c), for the load case 3, the stress value of the cable A10 in the mid-span of the side span approaches yielding stress. For the load case 4, the stress values of the cable in the area near the tower and the 1/4 region of the main span approach yielding stress, which are presented in Fig. 2(d). For the load cases 5 to 8, the cables are not yield, as presented in Fig. 2 (e) to 2(h).

The stress of the girder for the load cases 1 to 8 is presented in Fig.3. For the load case 1, as shown in Fig. 3(a), the stress in the mid-span area of the girder is yielding. For the load cases 2 and 3, the stress of the girder in the edge pier area is yielding, which is presented in Fig. 3(a). For the load case 4, the stress in the mid-span region of the girder is yielding, and the stress in the transition area between tower and beam also approaches the yielding stress, as shown in Fig. 3(a). As shown in Fig. 3(b), for the load cases 5 to 8, the stress of the main girder is at relatively low level.

The stress of the tower due to the load cases 1 to 8 is presented in Fig.4. As shown in Fig. 4(a), for the load case 1, the stress in middle tower columns and upper tower columns joint region is yielding. As presented in Fig. 4(a), for the load case 2, the stress in the middle of upper tower columns is relatively large. For the load case 3, the stress at the joint regions of the upper tower and the middle tower, and the joint region of the middle tower and the bottom tower are relatively large. For the load case 4, the stress at the end of bottom tower joint region approaches yielding stress. For the load case 5, the main stress in the joint region of the middle tower and upper tower approaches yielding stress, which is presented in Fig. 4(b). For the load case 6, the stress at the end of bottom tower approaches the yielding stress, and the stress in joint region of the middle tower and bottom tower also approaches yielding stress. For the load case 7, the stress in the joint region of the middle tower and the upper tower approaches the yielding stress. For the load case 8, the stress in the joint region of the middle tower and the bottom tower approaches yielding stress.

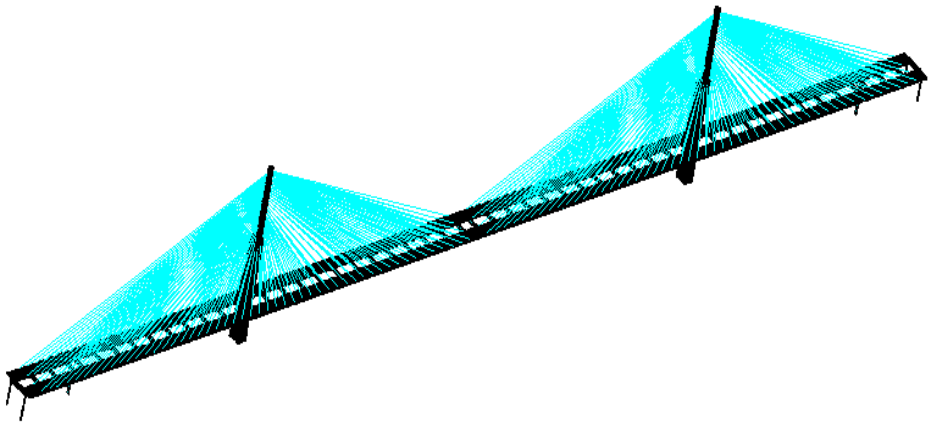

Fig. 1 The finite element model of the Bridge

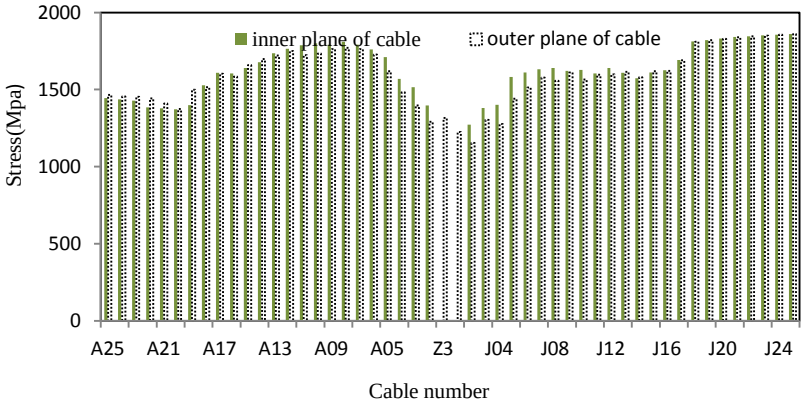

(a)

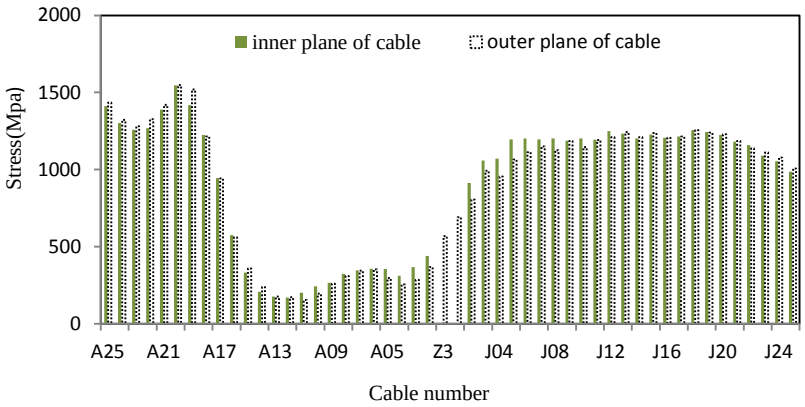

(b)

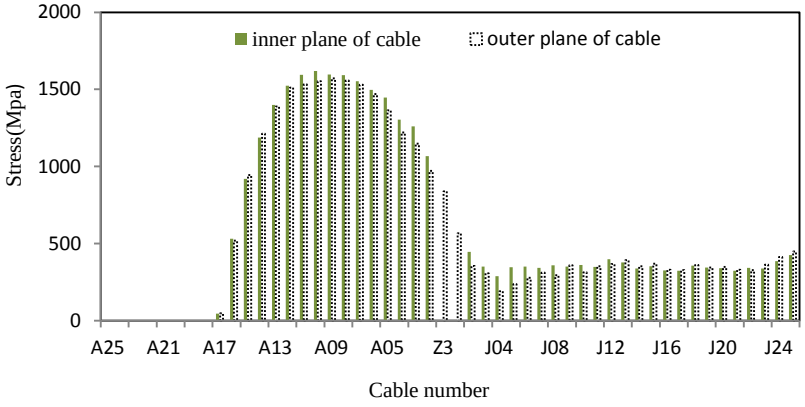

(c)

Continued-

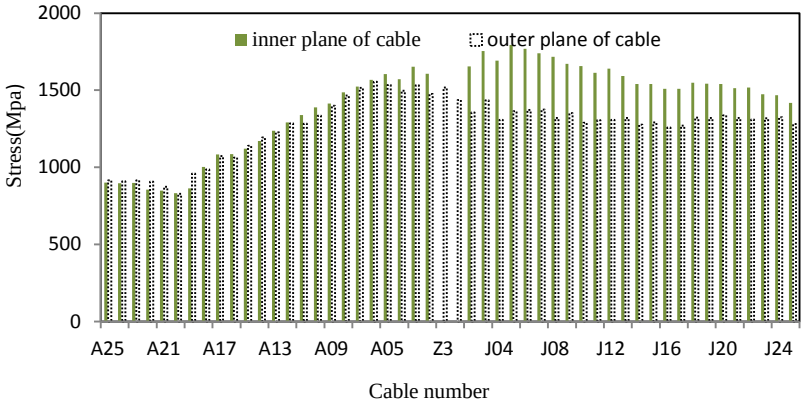

(d)

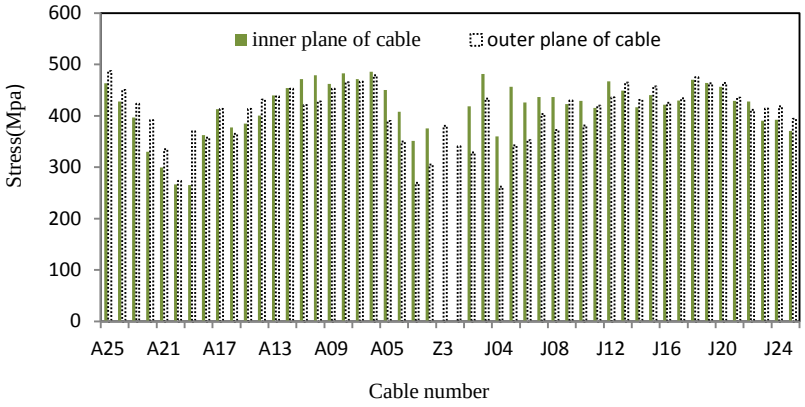

(e)

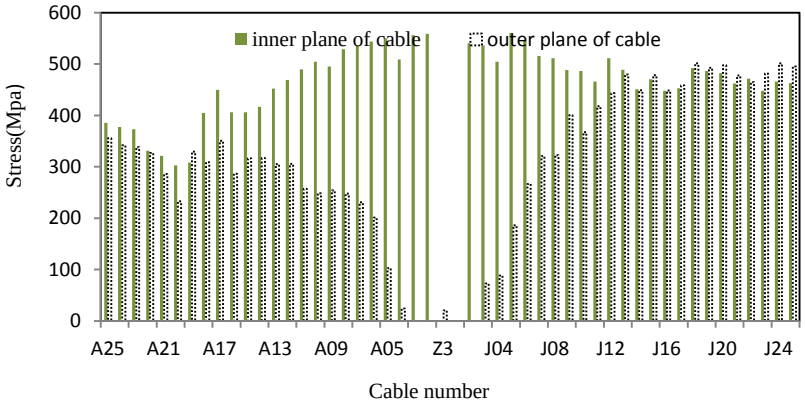

(f)

Continued-

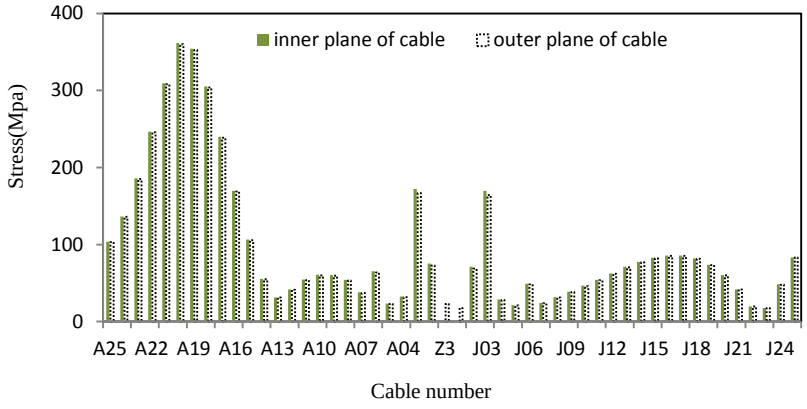

(g)

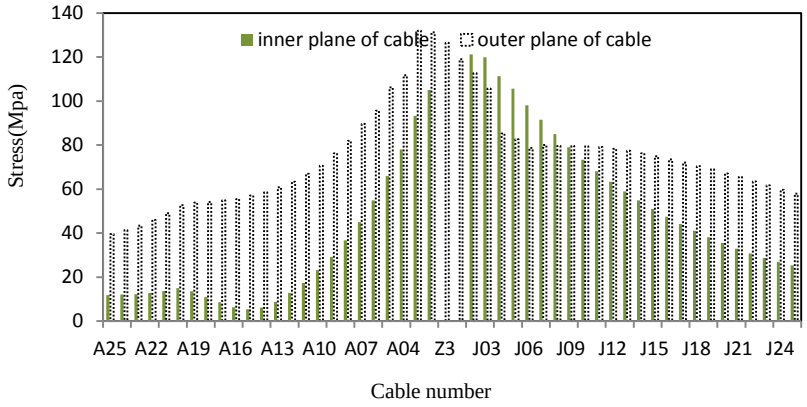

(h)

Fig. 2 The stress of cables for the eight load cases: (e) to (h)—Load cases 5 to 8

Table 1 Eight load cases

Load cases	Load description	Load cases	Load description
Case 1	Dead load +n× full bridge vehicle load	Case 5	Dead load + full bridge vehicle load + n×downwind load
Case 2	Dead load + n×main span vehicle load	Case 6	Dead load + full bridge vehicle load + n×crosswind load
Case 3	Dead load + n×side span vehicle load	Case 7	Dead load + n×E1 earthquake in longitudinal direction
Case 4	Dead load + n×one side vehicle load	Case 8	Dead load + n×E1 earthquake in transverse direction

3.4 Ultimate bearing capacity ratio, uniformity of the ultimate bearing capacity ratio, and reference ultimate bearing capacity ratio

In order to calculate the ultimate bearing capacity ratio of components, each element in the finite element model is assumed to be a component. The cable components, the girder components and the tower components are divided into three groups. For each load case, the ultimate bearing capacity ratio, the uniformity of the ultimate bearing capacity ratio, and the reference ultimate bearing capacity ratio of each set of components are calculated. Based on the results of ultimate bearing capacity analysis, the stress at the ultimate bearing state of each component can be obtained. The ultimate bearing capacity ratio, the uniformity of the ultimate bearing capacity ratio, and the reference ultimate bearing capacity ratio of each set of components are calculated for eight load cases.

Taking the load case 2 as an example, the ultimate bearing capacity ratio, the uniformity of the ultimate bearing capacity ratio, and the reference ultimate bearing capacity ratio of the cable component group, the girder component group and the tower component group are calculated respectively.

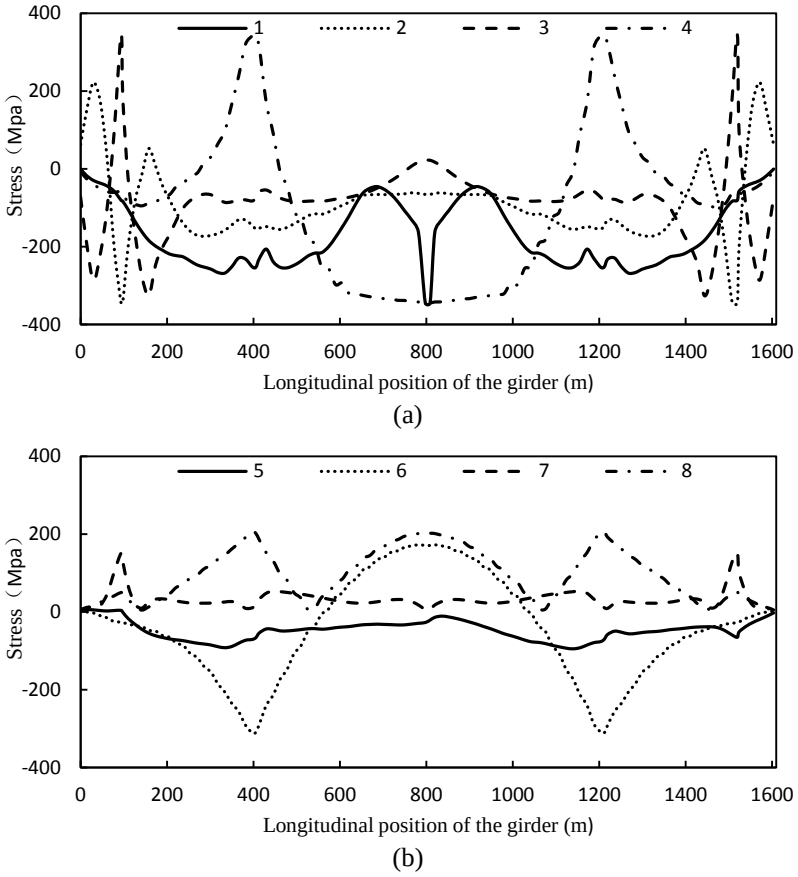

Fig. 3 The stress of the girder for the eight load cases: (a) load cases 1 to 4, and (b) load cases 5 to 8

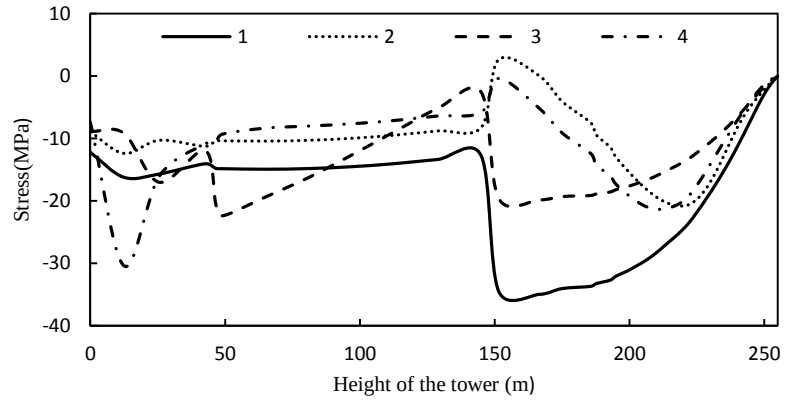

(a)

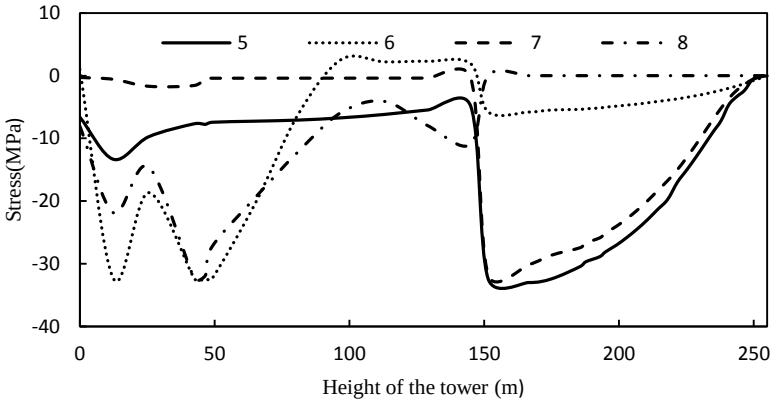

(b)

Fig. 4 The stress of the tower for the eight load cases: (a) load cases 1 to 4, and (b) load cases 5 to 8

Based on the ultimate bearing capacity ratio of the cable component group, the average ultimate bearing capacity ratio of the cable component group is calculated as $\bar{r}_{\lim}$ =0.49, the maximum ultimate bearing capacity ratio of the cable component group is calculated as $r_{\lim}^{\max}$ = 0.83, the minimum ultimate bearing capacity ratio of the cable group is calculated as $r_{\lim}^{\min}$ =0.08. Furthermore, the uniformity of the ultimate bearing capacity ratio of the cable component group is further calculated to be $d_{\lim}$ =0.43, as well as the reference ultimate bearing capacity ratio is $r_{\lim}^{0}$ =0.51.

Based on the ultimate bearing capacity ratio of the girder component group, the average ultimate bearing capacity ratio of the girder component group is calculated to be $\bar{r}_{\lim}$ =0.35, the maximum ultimate bearing capacity ratio of the girder component group is $r_{\lim}^{\max}$ =1.00, the minimum ultimate bearing capacity ratio of the girder component group is $r_{\lim}^{\min}$ =0.02. Furthermore, the uniformity of the ultimate bearing capacity ratio of the girder component group is further calculated to be $d_{\lim}$ =0.35, as well as the reference ultimate bearing capacity ratio is $r_{\lim}^{0}$

=0.73.

Based on the ultimate bearing capacity ratio of the tower component group, the average ultimate bearing capacity ratio of the tower component group is calculated to be $\bar{r}_{\lim}$ =0.23, the maximum ultimate bearing capacity ratio of the tower component group is $r_{\lim}^{\max}$ =0.58, the minimum ultimate bearing capacity ratio of the tower component group is $r_{\lim}^{\min}$ =0.01. Furthermore, the uniformity of the ultimate bearing capacity ratio of the tower component group is further calculated to be $d_{\lim}$ =0.29, as well as the reference ultimate bearing capacity ratio is $r_{\lim}^{0}$ =0.42.

The ultimate bearing capacity ratio of the cables from A1 to A25, J1 to J25, A'2 to A'25 and J'2 to J'25, the 1/2 span the girder, and Z3 tower are further presented in table 2.

Based on the above analysis, the reference ultimate bearing capacity ratio of the cable component group, the girder component group, and the tower component group are calculated and presented in table 3. When the component ultimate bearing capacity ratio is equal to 1, the failure of the component is indicated.

4. Internal force monitoring design for the second highway bridge of Wuhu Yangtze river

In this section, the internal force monitoring components are designed based on the component ultimate bear capacity ratio.

4.1 Cable force monitoring

For the load case 1, the high bearing components of the cables are the cables in the edge pier area, the mid-span region of the side span, the 1/4 region of the main span, and the mid-span region of the main span. In the edge pier area, the ultimate bearing capacity ratio of the cable A25 in the outer cable plane is 0.79. The ultimate bearing capacity ratio of the cable A'25 in the inner cable plane is 0.78. In the mid-span region of side span, the ultimate bearing capacity ratio of the cable A10 in the outer cable plane is 0.93. The ultimate bearing capacity ratio of the cable A'10 in the inner cable plane is 0.97. In the 1/4 region of the main span, the ultimate bearing capacity ratio of the cable J12 in the outer cable plane is 0.86. The ultimate bearing capacity ratio of the cable J'12 in the inner cable plane is 0.88. In the mid-span region of the main span, the ultimate bearing capacity ratio of the cable J25 in the outer cable plane and the stay cable J'25 in the inner cable plane are equal to 1.

For the load case 2, the high bearing components of the cables are the cables in the edge pier area, the auxiliary pier area, and the 1/4 region of the main span. In the edge pier area, the ultimate bearing capacity ratio of the cable A25 in the outer cable plane is 0.77. The ultimate bearing capacity ratio of the cable A'25 in the inner cable plane is 0.76. In the auxiliary pier area, the ultimate bearing capacity ratio of the cable A20 in the outer cable plane is 0.76. The ultimate bearing capacity ratio of the cable A'20 in the inner cable plane is 0.83. In the 1/4 region of the main span, the ultimate bearing capacity ratio of the cable J12 in the outer cable plane is 0.65. The ultimate bearing capacity ratio of the cable J'12 in the inner cable plane is 0.67.

Table 2 Ultimate bearing capacity ratio of the components

	Cable component group (Cable numbers : A1 to A25, J1 to J25, A'2 to A'25 and J'2 to J'25)	Girder component group (The components of 1/2 span the girder)	Z3 tower component group
Ultimate bearing capacity ratio	0.31、0.20、0.15、0.14、0.16、0.19、0.18、0.17、0.14、0.10、0.08、0.09、0.09、0.13、0.19、0.30、0.51、0.65、0.82、0.83、0.76、0.71、0.69、0.71、0.77、0.37、0.43、0.53、0.51、0.57、0.60、0.62、0.60、0.64、0.62、0.64、0.65、0.67、0.65、0.67、0.65、0.65、0.68、0.67、0.66、0.64、0.61、0.60、0.58、0.54、0.24、0.20、0.17、0.19、0.19、0.19、0.17、0.14、0.13、0.11、0.09、0.09、0.11、0.18、0.31、0.51、0.66、0.76、0.83、0.75、0.68、0.68、0.70、0.76、0.49、0.57、0.58、0.64、0.65、0.64、0.65、0.64、0.65、0.64、0.67、0.66、0.65、0.66、0.65、0.65、0.67、0.67、0.66、0.64、0.62、0.59、0.57、0.53	0.18、0.43、0.64、0.50、0.07、0.58、1.00、0.99、0.59、0.25、0.04、0.15、0.02、0.13、0.23、0.33、0.41、0.46、0.49、0.50、0.50、0.48、0.46、0.42、0.38、0.38、0.42、0.45、0.44、0.43、0.44、0.45、0.44、0.41、0.38、0.35、0.34、0.34、0.32、0.30、0.27、0.25、0.22、0.20、0.19、0.19、0.19、0.19、0.19、0.19、0.18、0.18、0.19	0.28、0.38、0.32、0.35、0.32、0.32、0.32、0.31、0.29、0.27、0.25、0.15、0.00、0.13、0.23、0.29、0.35、0.40、0.46、0.52、0.56、0.60、0.63、0.64、0.64、0.61、0.55、0.48、0.40、0.31、0.24、0.17、0.12、0.08、0.03、0.01

Table 3 Reference ultimate bearing capacity ratio and failure components

Load cases	Cable	Girder	Tower	Failure components and areas
Case 1	0.70	0.67	0.64	The cable at mid-span, joint region of the middle tower and the upper tower
Case 2	0.51	0.73	0.42	Girder component at the auxiliary pier area
Case 3	0.64	0.76	0.68	Girder component at the auxiliary pier area
Case 4	0.62	0.66	0.45	Girder component at the transition area between tower and girder, the midspan region of the girder
Case 5	0.18	0.18	0.76	Joint region of the middle tower and the upper tower
Case 6	0.28	0.72	0.75	Joint region of the middle tower and bottom tower , the end of bottom tower region
Case 7	0.25	0.35	0.78	Joint region of the middle tower and bottom tower
Case 8	0.14	0.40	0.82	Joint region of the middle tower and the bottom tower

For the load case 3, the high bearing components of the cables is the cables in the mid-span region of side span. In the mid-span region of side span, the ultimate bearing capacity ratio of the cable A10 in the outer cable plane is 0.84. The ultimate bearing capacity ratio of the cable A'10 in

the inner cable plane is 0.87.

For the load case 4, the high bearing components of the cables are cables in the area near the tower and the 1/4 region of the main span. In the area near the tower, the ultimate bearing capacity ratio of the cable A1 in the outer cable plane is 0.82. In the 1/4 region of the main span, the ultimate bearing capacity ratio of the cable J'12 in the inner cable plane is 0.88.

For the load cases 5 to 8, the bearing capacity of the cable is relatively low. Based on the above analysis, the maximum ultimate bearing capacity ratios of the cables for load cases 1 to 4 are further presented in Table 4. The cables at the position of the edge pier, the cables at the position of auxiliary pier, the cables at the position of the mid-span of the side span, the cables at the position of the tower, and the cables at the position of the 1/4 of the main span and the mid-span of the main span are finally designed to be monitored components. Total 48 cables are monitored. The cable monitoring position is further shown in Fig. 5.

4.2 Stress monitoring of the girder

For the load case 1, the high bearing components of the girder are the girder element in the transition area between tower and beam, and the mid-span region of the main span. The ultimate bearing capacity ratio of the girder component in the mid-span of the main span is 0.98.

For the load case 2, the high bearing components of the girder are the girder elements above the auxiliary pier area. The ultimate bearing capacity ratio of the girder component above the auxiliary pier is equal to 1.

For the load case 3, the high bearing components of the girder are the girder elements above the auxiliary pier area. The ultimate bearing capacity ratio of the girder component above the auxiliary pier is equal to 1.

For the load case 4, the high bearing components of the girder are girder elements in the transition area between tower and girder, and the mid-span region of the main span. The ultimate bearing capacity ratio of the girder component in the transition area between tower and girder and the mid-span of the main span are equal to 1.

For the load case 6, the high bearing components of the girder are girder elements in the transition area between tower and girder. The ultimate bearing capacity ratio of the girder component in the transition between tower and beam is 0.90.

For the load cases 5, 7 and 8, the bearing capacity ratio of the girder component are at relatively low level. The component ultimate bearing capacity ratios of the high bearing components of the girder are presented in Table 5. Based on the above analysis, the stress monitoring sections of the girder includes: the girder cross sections at the mid-span of the main span, the transition section between tower and girder, and the junction of pier and girder. The stress monitoring sections of the girder are further shown in Fig. 6.

4.3 Stress monitoring of the tower

For the load case 1, the high bearing components of the tower are the tower joint components of the middle tower and the upper tower. The ultimate bearing capacity ratio of the component is equal to 1.

For the load case 2, the high bearing components of the tower are the joint components in the region of the middle tower and the upper tower. The ultimate bearing capacity ratio of the component is 0.64.

Table 4 Ultimate bearing capacity ratios of high bearing components of the cables

Load cases	The edge pier area	The auxiliary pier area	The mid-span region of the side span	The transition area between tower and beam	The 1/4 region of the main span	The mid-span region of the main span
Case 1	0.76~0.79	--	0.92~0.97	--	0.84~0.88	1.00
Case 2	0.69~0.77	0.65~0.83	--	--	0.62~0.67	--
Case 3	--	--	0.65~0.87	--	--	--
Case 4	--	--	0.72~0.82	--	0.69~0.88	--

Table 5 Ultimate bearing capacity ratios of high bearing components of the girder

Load cases	The auxiliary pier area	The transition area between tower and beam	The mid-span region of the main span
Case 1	--	0.69~0.78	0.98
Case 2	0.99~1.00	--	--
Case 3	0.94~1.00	--	--
Case 4	--	0.93~1.00	0.94~1.00
Case 6	--	0.74~0.90	--

For the load case 3, the high bearing components of the tower are the joint components in the region of the middle tower and the upper tower, the joint components of the middle tower and the bottom tower. The ultimate bearing capacity ratios of these two components are equal to 0.61 and 0.71, respectively.

For the load case 5, the high bearing component of the tower is the bottom component of the tower. The ultimate bearing capacity ratio is 0.94.

For the load case 5, the high bearing component of the main tower is the joint component in the region of the middle tower and the upper tower. The ultimate bearing capacity ratio is equal to 1.

For the load case 6, the high bearing components of the main tower are the components in the bottom tower, the joint region of the middle tower and the bottom tower. The ultimate bearing capacity ratio of the bottom tower, and the joint component of the middle tower and bottom tower are equal to 1.

For the load case 7, the high bearing component of the tower is the joint component of in the region of the middle tower and the upper tower. The ultimate bearing capacity ratio is equal to 1.

For the load case 8, the high bearing component of the tower is the joint component in the region of the middle tower and the bottom tower. The ultimate bearing capacity ratio is equal to 1.

The component ultimate bearing capacity ratio of the high bearing components of the tower are further presented in Table 6. Based on the above analysis, the stress monitoring sections of the tower includes: the joint component in the region of the middle tower and the upper tower, the joint component in region of the middle tower and the bottom tower, and the bottom of the tower. The stress monitoring sections of the tower are further presented in Fig. 7.

Finally, the number of monitoring components is summarized in Table 7. As one can seen from Table 7, the internal forces of the structure are monitored with a total of 59 components.

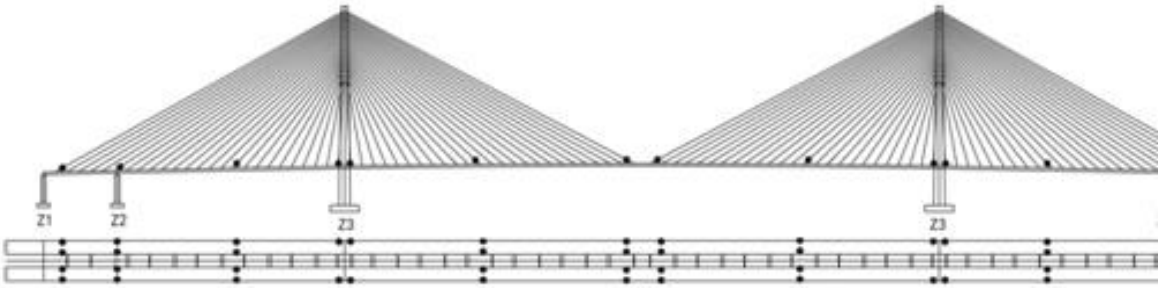

Fig. 5 Layout of cable force monitoring points

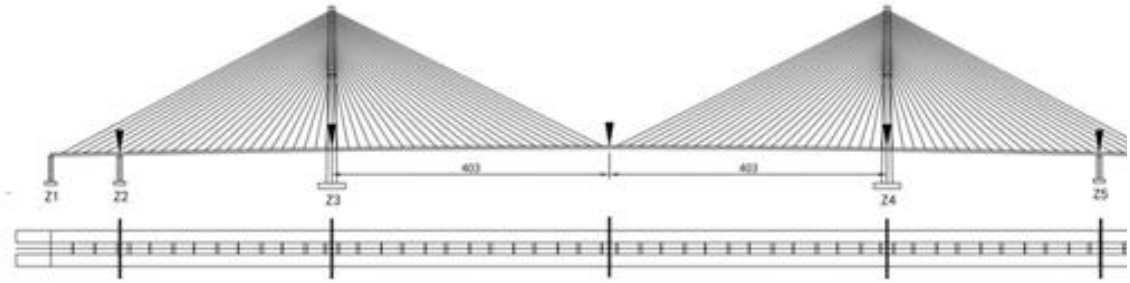

Fig. 6 Layout of stress monitoring sections of the girder

Table 6 Ultimate bearing capacity ratios of high bearing components of the tower

Load cases	The end of bottom tower columns joint region	Middle tower columns and bottom tower columns joint region	Middle tower columns and upper tower columns joint region
Case 1	--	--	0.67~1.00
Case 3	--	0.63~0.71	0.59~0.61
Case 4	0.94	--	--
Case 5	--	--	1.00
Case 6	1.00	0.97~1.00	--
Case 7	--	--	0.80~1
Case 8	--	0.84~1	--

Table 7 Internal force monitoring Components

	Monitoring contents	Numbers
1	Cable force	48 cables
2	Sress of the girder	5 sections
3	Stress of the tower	6 sections

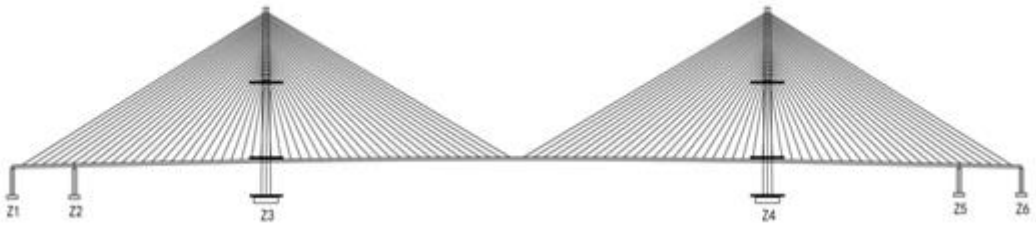

Fig. 7 Layout of stress monitoring sections of the two Tower

5. Conclusions

This paper proposed a novel internal force monitoring design method for long span bridges based on the ultimate bearing capacity ratios of the structural components. The proposed method is finally applied into the second bridge of Wuhu Yangtze river. Based on this research, the following conclusion can be drawn,

- The proposed method is based on the ultimate bearing capacity of long-span bridges subjected to various load cases. Based on the ultimate bearing capacity of the structural component, the component ultimate bearing capacity ratio, the uniformity of ultimate bearing capacity ratio, and the reference of component ultimate bearing capacity ratio are defined. Through the quantitative analysis of the bearing capacity of the components, the high bearing components of the bridge structure can then be determined as the monitoring components. The proposed method can provide quantitative criteria for bridge internal force monitoring design.
- The monitoring components based on the proposed method are consistent with the actual failure process of the bridge, and can reduce the monitoring of low bearing components. For the second highway bridge of Wuhu Yangtze river, 59 components are designed to be monitored. Therefore, the bridge internal force monitoring design based on the ultimate bearing capacity ratio can decrease the components and the cost of monitoring system.
- The proposed method is limited to the internal force monitoring design of the bridge structure. The whole health monitoring system of bridge also includes other monitoring indicators, such as structural characteristics, structural loads monitoring indicators and so on.

Acknowledgements

The authors would like to thank the financial supports by the National Natural Science Foundation of China under grand No. 51578206, by "The Fundamental Research Funds for the Central Universities", by the Natural Science Funds for Distinguished Young Scholar of Anhui province under grand No, 1708085J06, and by the National Key R&D Program of China under grand no. 2017 YFC 0805100.

References

Boller, C. (2009), *Encyclopedia of Structural Health Monitoring*, John Wiley and Sons, Ltd., United Kingdom.

Brownjohn, James, M.W., Kripakaran, P., Harvey, B., Kromanis, R., Jones, P. and Huseynov, F. (2016), "Structural heath monitoring of short to medium span bridges in the United Kindom", *Struct. Monit. Maint.*, **3**(3), 259-276.

Bruno, D. and Grimaldi, A. (1985), "Nonlinear behaviour of long-span cable-stayed bridges", *Meccanica*, **20**(4), 303-313.

Fish, P.E. and Prine, D.W. (1996), "Fracture critical inspection and global remote monitoring of Michigan street lift bridge", *Proceedings of the Structural Materials Technology. An NDT Conference*, San Diego, USA, February.

Hong, D.S. and Kim, J.T. (2010), " Structural health monitoring of full-scale concrete girder bridge using acceleration response", *J. Korea Inst. Struct. Maint. Inspection*, **14**(1), 165-174.

Housner, G.W., Bergman, L.A., Caughey, T.K., Chassiakos, A.G., Claus, R.O. and Masri, S.F. (1997), "Special issue, structural control: past, present and future", *J. Eng. Mech*., **123**(9), 897-971.

Kister, G., Winter, D., Badcock, R.A., Gebremichael, Y.M., Boyle, W.J.O. and Meggitt, B.T. (2007), "Structural health monitoring of a composite bridge using bragg grating sensors. part 1: evaluation of adhesives and protection systems for the optical sensors", *Eng. Struct*., **29**(3), 440-448.

Kister, G., Winter, D., Tetlow, J., Barnes, R., Mays, G. and Fernando, G.F. (2005), "Structural integrity monitoring of reinforced concrete structures. part 1: evaluation of protection systems for extrinsic fibre fabry–perot sensors", *Engineering Structures*, **27**(3), 411-419.

Li, H.N. and Li, D.S. (2002), "Safety assessment, health monitoring and damage diagnosis for structures in civil engineering", *Earthq. Eng. Eng. Vib*., **22**(3), 82-90.

Li, H.N., Li, D.S., Ren, L., Yi, T.H., Jia, Z.G. and Li, K.P. (2016), "Structural health monitoring of innovative civil engineering structures in Mainland China", *Struct. Monit. Maint.*, **3**(1), 1-32.

Nazmy, A.S. (2003), "Seismic response analysis of long-span steel arch bridges", *J. Bridge Eng*., **156**(2), 91-97.

Nazmy, A.S. and Abdel-Ghaffar, A.M. (1990), "Non-linear earthquake response analysis of long-span cable-stayed bridges: theory", *Earthq. Eng. Struct. D*., **19**(1), 63-76.

Ren, W.X. (1999), "Ultimate behavior of long-span cable-stayed bridges", *J. Bridge Eng*., **4**(1), 30-37.

Ren, W.X. and Obata, M. (1999), "Elastic-plastic seismic behavior of long span cable-stayed bridges", *J. Bridge Eng*., **4**(3), 194-203.

Roschke, P.N. and Pruski, K.R. (2000). "Overload and ultimate load behavior of posttensioned slab bridge", *J. Bridge Eng*., **5**(2), 148-155.

Sloan, T.D., Kirkpatrick, J., Boyd, J.W. and Thompson, A. (1992), "Monitoring the inservice behaviour of the foyle bridge", *Struct. Engineer*, **70**, 130-134.

Sun, L., Sun, Z. and Yu, G. (2006), "Bridge vulnerability analysis based health monitoring system design", Iabse Symposium Report, Copenhagen, Denmark, January.

Sun, L.M. and Yu, G. (2010), "Vulnerability analysis for design of bridge health monitoring system", *Proceedings of SPIE - The International Society for Optical Engineering*, **37**(3),76502K-76502K-9.

Yi, T.H., Li, H.N. and Gu, M. (2011), "Optimal sensor placement for structural health monitoring based on multiple optimization strategies", *Struct. Des. Tall Spec. Build*., **20**(7), 881-900.

Yi, T.H., Li, H.N. and Gu, M. and Zhang, X.D. (2014), "Sensor placement optimization in structural health monitoring using niching monkey algorithm", *Int. J. Struct. Stab. Dynam*., **14**(5), 1440012.

Yi, T.H., Li, H.N. and Zhang, X.D. (2012), "A modified monkey algorithm for optimal sensor placement in structural health monitoring", *Smart Mater. Struct*., **21**(10), 52-53.